Colliders and Collider Physics at the Highest Energies
Muon Colliders at 10 GeV to 100 TeV
HEMC'99 Workshop, Montauk, New York 1999
Editor B.J. King, AIP Conference Proceedings Vol.530, 2000. pp. 217-227.

Effects of Kinematic Correction on the Dynamics in Muon Rings

Kyoko Makino and Martin Berz

Department of Physics and Astronomy and
National Superconducting Cyclotron Laboratory
Michigan State University, East Lansing, MI 48824, USA

Abstract. Among many other challenges faced by muon accelerators and storage rings, the influence of nonlinear effects has to be studied carefully compared to conventional proton and electron machines. The short lifetime of muons as well as their production mechanism make the cooling of muon beams a necessity; however, in many scenarios still rather large transversal emittances persist, which makes nonlinear effects more pronounced than usual.

There are a variety of sources for nonlinear effects besides deliberate and random nonlinear multipoles; particularly, there are nonlinear effects due to fringing fields, which have been known in the design of high-resolution spectrographs and recently have also been studied for storage rings [1]. Details of some first estimates of their effects are given in an accompanying paper [2]. In this paper we address another nonlinear effect that is directly connected to the presence of large emittances, namely the so-called kinematic correction, and report first results of the effects on some current muon storage ring designs.

INTRODUCTION

The most general form of the Hamiltonian of a charged particle in electromagnetic fields in curvilinear coordinates $\{s, x, y\}$ can be written in terms of the generalized momentum $\vec{P}^G = (P_s^G, P_x^G, P_y^G)$ as [3]

$$H = q\Phi + c\sqrt{\frac{(P_s^G + P_x^G\tau_1 y - P_y^G\tau_1 x - \alpha q A_s)^2}{\alpha^2} + (P_x^G - qA_x)^2 + (P_y^G - qA_y)^2 + m^2c^2}. \quad (1)$$

Here, τ_1 is the rate of rotation around the beam axis, τ_2 and τ_3 are curvatures in y-s and x-s planes, and α is defined as $\alpha = 1 - \tau_3 x + \tau_2 y$. The generalized momentum is expressed in terms of the kinematic momentum $\vec{p} = (p_s, p_x, p_y)$, where we usually expect $p_s^2 \gg p_x^2, p_y^2$, as

$$P_s^G = (p_s + qA_s)\alpha - (p_x + qA_x)\tau_1 y + (p_y + qA_y)\tau_1 x$$
$$P_x^G = p_x + qA_x, \quad P_y^G = p_y + qA_y.$$

Apparently the first term in the square root in the Hamiltonian (1) is the leading term, and the approximation to omit the second and the third terms, which entail nonlinear effects purely due to dynamics and independent of the fields, is widely used.

In case of muon accelerators and storage rings and their typically large transversal emittances, p_x and p_y are not safely negligible compared to p_s anymore. The restoration of those omitted terms is often referred to as kinematic correction, and the effects of the kinematic correction as well as the other nonlinear effects have to be studied and treated more seriously for muon machines than for conventional proton and electron machines.

COSY INFINITY

The code COSY INFINITY [4] is a transfer map based beam physics code working to arbitrary high order [5,6]. All nonlinear terms are included in the necessary equations from the outset, and the nonlinear effects can be taken care of up to any desired order.

As shown in [3], particles following x-s planar motion, in which case $(\tau_1, \tau_2, \tau_3) = (0, 0, -h)$, obey the following set of equations of motion [7]:

$$x' = a(1+hx)\frac{p_0}{p_s} \tag{2a}$$
$$y' = b(1+hx)\frac{p_0}{p_s} \tag{2b}$$
$$a' = \left\{(1+\delta_m)\frac{1+\eta}{1+\eta_0}\frac{p_0}{p_s}\frac{E_x}{\chi_{E0}} - \frac{B_y}{\chi_{M0}} + b\frac{p_0}{p_s}\frac{B_s}{\chi_{M0}}\right\}(1+hx)(1+\delta_z) + h\frac{p_s}{p_0} \tag{2c}$$
$$b' = \left\{(1+\delta_m)\frac{1+\eta}{1+\eta_0}\frac{p_0}{p_s}\frac{E_y}{\chi_{E0}} + \frac{B_x}{\chi_{M0}} - a\frac{p_0}{p_s}\frac{B_s}{\chi_{M0}}\right\}(1+hx)(1+\delta_z), \tag{2d}$$

Here $m = m_0(1+\delta_m)$, $q = z_0 e(1+\delta_z)$, with the index $_0$ expressing the respective quantities of the reference particle. We use the quantities $a = p_x/p_0$ and $b = p_y/p_0$. Furthermore,

$$\chi_{E0} = \frac{p_0 v_0}{z_0 e}, \quad \chi_{M0} = \frac{p_0}{z_0 e}, \quad \eta = \frac{K_0(1+\delta_k) - z_0 e(1+\delta_z)V(x,y,s)}{m_0 c^2(1+\delta_m)}$$

and

$$\frac{p_s}{p_0} = \sqrt{(1+\delta_m)^2\frac{\eta(2+\eta)}{\eta_0(2+\eta_0)} - a^2 - b^2}. \tag{3}$$

In this expression, the kinematic correction terms in the Hamiltonian, the second and the third terms in the square root in (1), correspond to the terms a^2 and b^2 in the square root in (3). Note that the kinematic correction appears from the second order in p_s/p_0 and hence in p_0/p_s. The expression p_s/p_0 appears in all equations (2a) to (2d). The B_y term in a' and the B_x term in b' are leading terms in (2c) and (2d), so the first kinematic correction effect may appear from the $h \cdot p_s/p_0$ term in a', and thus produce second order effects for x and a, and third order effects for y and b. The correctness of the appearing higher order kinematic correction terms was verified in [8].

COSY INFINITY includes kinematic correction routinely without any approximation as indicated in the equations (2a) to (2d) and (3). In order to study the effects of kinematic correction, which is frequently omitted in other codes, an option was created that ignores the terms a^2 and b^2 in the square root in (3). In the following, computational results were obtained by COSY INFINITY by using its default set of equations and by using a similar set of equations with kinematic correction turned off.

KINEMATIC CORRECTION IN MUON STORAGE RINGS

In the following we present observations related to the kinematic correction effects. We limit ourselves to the mere observation of the effects, without attempting to devise strategies for their correction through nonlinear elements, which of course should also include the influence of all other relevant nonlinear effects.

We studied the same muon storage rings as the ones used in [2]. This section reports on the effects on the 30 GeV neutrino factory ring and the 30 GeV Higgs factory ring.

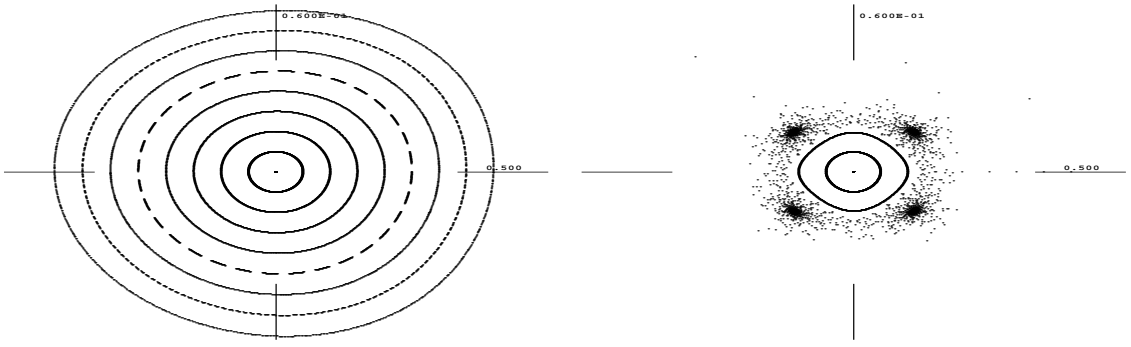

FIGURE 1. Tracking pictures for 1000 turns in a 30 GeV neutrino factory ring without (left) and with (right) kinematic correction in the same scale of 500mm×60mrad. With correction, only those particles up to 100mm×15mrad are stable.

TABLE 1. The beginning part of the Taylor transfer map of a 30 GeV neutrino factory ring without kinematic correction.

Expansion coefficients of x,a,y,b depending on the exponents of xayb

(x,	(a,	(y,	(b,	xayb
-0.1936744	0.1416905	0	0	1000
-6.792904	-0.1936744	0	0	0100
0	0	0.1961760	-0.2456274E-01	0010
0	0	39.14526	0.1961760	0001
0.5590897E-01	-0.1884921E-02	0	0	2000
-0.2374424	-0.7032995E-01	0	0	1100
-0.9129287	-0.4467585	0	0	0200
0	0	0.1229122	-0.3076403E-03	1010
0	0	0.6994628	0.2591721E-02	0110
0	0	-0.4902813	-0.1229122	1001
0	0	4.130383	-0.6994626	0101
-0.8336143E-02	-0.1539706E-02	0	0	0020
0.2386714	0.1206977E-01	0	0	0011
13.28519	2.453805	0	0	0002
-0.3176306E-01	0.9418167E-03	0	0	3000
0.1598218	0.3223752E-01	0	0	2100
1.083413	-0.9744992E-01	0	0	1200
0.6192792	-1.809375	0	0	0300
0	0	0.4798076E-02	0.2628223E-03	2010
0	0	0.1013059	0.9227448E-02	1110
0	0	2.193448	0.1482136E-02	0210
0	0	0.5991117	0.5041080E-01	2001
0	0	21.11926	-0.4081118E-01	1101
0	0	2.237190	0.3706776	0201
-0.2023107E-02	-0.4458563E-03	0	0	1020
-0.2897106E-02	-0.8739436E-02	0	0	0120
-0.1355373	-0.6453340E-01	0	0	1011
-2.883894	-0.1806350E-01	0	0	0111
-10.94397	0.9968734E-01	0	0	1002
26.07000	-0.2402591	0	0	0102
0	0	0.8583696E-03	0.3180518E-05	0030
0	0	-0.1950716E-01	-0.9494305E-03	0021
0	0	-1.513093	0.1950715E-01	0012
0	0	-8.077975	1.367970	0003
0.1285578E-01	-0.1272996E-03	0	0	4000
.....	.....	.....	.....	....

TABLE 2. The beginning part of the Taylor transfer map of a 30 GeV neutrino factory ring with kinematic correction.

Expansion coefficients of x,a,y,b depending on the exponents of xayb

(x,	(a,	(y,	(b,	xayb
-0.1936744	0.1416905	0	0	1000
-6.792904	-0.1936744	0	0	0100
0	0	0.1961760	-0.2456274E-01	0010
0	0	39.14526	0.1961760	0001
0.9450713E-01	0.3330788E-02	0	0	2000
0.1377180	-0.5612056E-01	0	0	1100
-0.5801038	-0.6286416	0	0	0200
0	0	0.1229122	-0.3076403E-03	1010
0	0	0.6994628	0.2591721E-02	0110
0	0	-0.4902813	-0.1229122	1001
0	0	4.130383	-0.6994626	0101
-0.8336143E-02	-0.1539706E-02	0	0	0020
0.2386714	0.1206977E-01	0	0	0011
13.28519	2.453805	0	0	0002
11.55775	-0.1950424	0	0	3000
-81.95874	4.704898	0	0	2100
392.7585	-40.95482	0	0	1200
-1667.934	610.1026	0	0	0300
0	0	-0.7719322	-0.4832862E-01	2010
0	0	14.24336	0.4605147	1110
0	0	-417.3649	-2.944554	0210
0	0	-6.277132	-8.007910	2001
0	0	354.6553	34.10640	1101
0	0	-782.7162	-69.64528	0201
0.2344129	-0.2585728E-01	0	0	1020
-3.593587	1.490467	0	0	0120
26.50950	-1.496885	0	0	1011
-116.8393	6.467636	0	0	0111
2245.991	-29.01786	0	0	1002
-4789.016	244.2371	0	0	0102
0	0	-1.130680	-0.7756062E-02	0030
0	0	-6.403961	-0.4518258	0021
0	0	-430.3112	-29.87579	0012
0	0	-1116.550	-1705.361	0003
-1.322453	-0.9516536E-01	0	0	4000
.....	.....	.....	.....	....

TABLE 3. Amplitude dependent tune shifts.

Kinematic correction		off	on		Order	Exponents	
Fringe field effects		off		on		x	y
30 GeV neutrino factory ring	x motion	0.718979	0.718979	0.718979	0	0	0
		-0.0228772	12.0363	469.397	2	2	0
		-0.0305743	5.32077	741.941	2	0	2
	y motion	0.218573	0.218573	0.218573	0	0	0
		-0.0305743	5.32077	741.941	2	2	0
		-0.0071152	5.92760	472.150	2	0	2
30 GeV Higgs factory ring	x motion	0.864288	0.864288	0.864288	0	0	0
		-0.837791	35.8432	855.939	2	2	0
		-1.76978	42.0333	2226.02	2	0	2
	y motion	0.665356	0.665356	0.665356	0	0	0
		-1.76978	42.0333	2226.02	2	2	0
		-0.225010	422.116	4180.00	2	0	2

The neutrino factory ring consists of bending elements and quadrupoles, and the Higgs factory ring furthermore has sextupoles. Tables 1 and 2 show the beginning part of high order Taylor transfer maps of the neutrino factory ring. Table 1 shows the case without kinematic correction, and Table 2 the case with kinematic correction, which is obtained as the default of COSY INFINITY. As expected from the discussion in the previous section, the effects start to appear from the second order in x and a, and from the third order in y and b.

The size of the dynamic aperture was estimated by tracking particles for 1000 turns with transfer maps up to 7th order. In case of no kinematic correction, particles with x up to 1000mm and a up to 150mrad are stable in the neutrino factory ring. However when the kinematic correction is included, the particles with x up to 100mm and a up to 15mrad are stable. Figure 1 illustrates how the particles are preserved in case the kinematic correction is on in the right picture in comparison to the case without correction in the left picture, where the particles look very stable.

Based on normal form methods, amplitude dependent tune shifts were computed using COSY INFINITY [9,10]. Table 3 summarizes the results with and without kinematic correction; in addition, the effects of fringing fields are listed for comparison [2], where the full gap size of the magnets is assumed to be 10cm and the standard Enge function is used to describe the fall-off of the field at each fringing region [4].

The pictures in Figure 2 show tune footprints of the neutrino factory ring for particles up to 6mm in radius in both x and y directions. The horizontal axis shows the x tune and the vertical shows the y tune. The upper picture shows the tune footprint without kinematic correction. The lower picture shows the two footprints with and without correction in the same scale; the small dark spot at the lower left is the one without correction.

Altogether, for the design of the neutrino factory ring used in the study, the

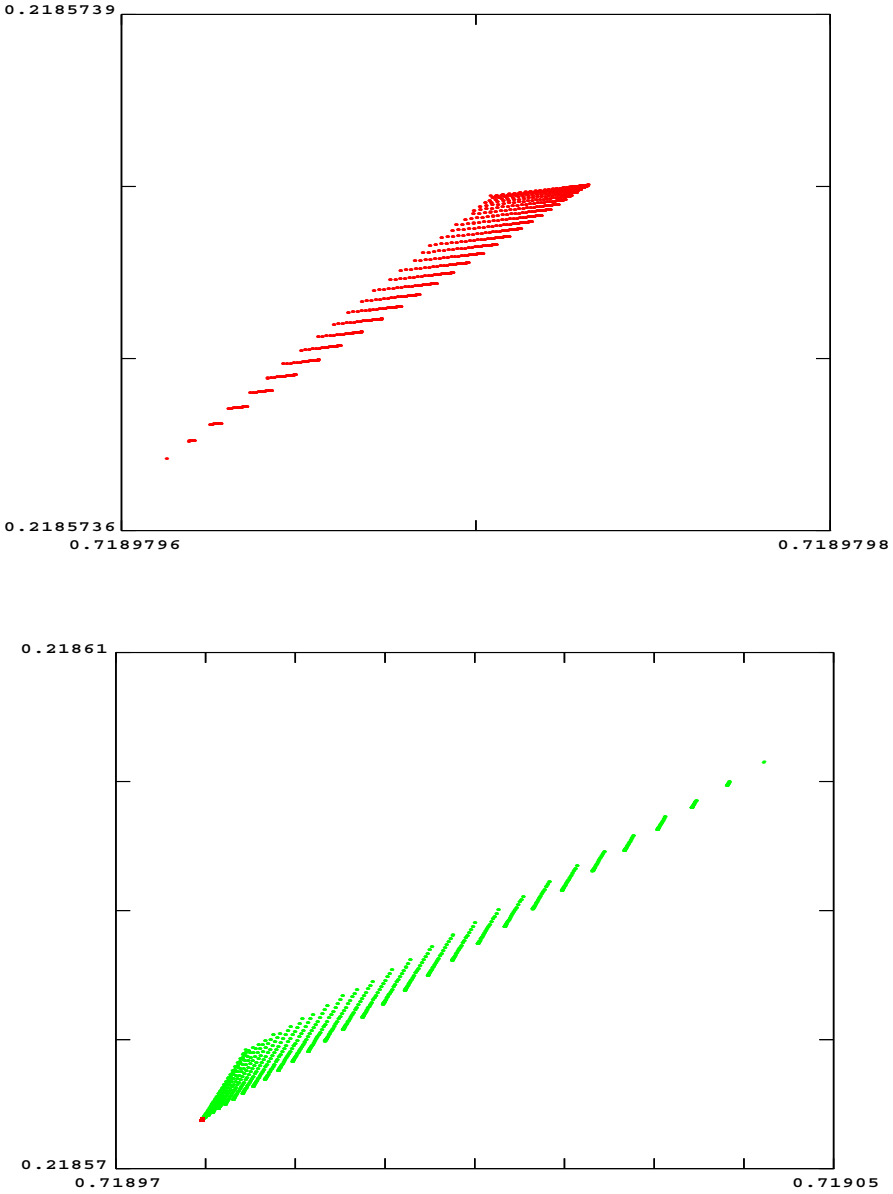

FIGURE 2. Tune footprints of a 30 GeV neutrino factory ring without (upper) and with kinematic correction. The lower picture shows both in the same scale, where the one without correction is the tiny dark spot at the lower left.

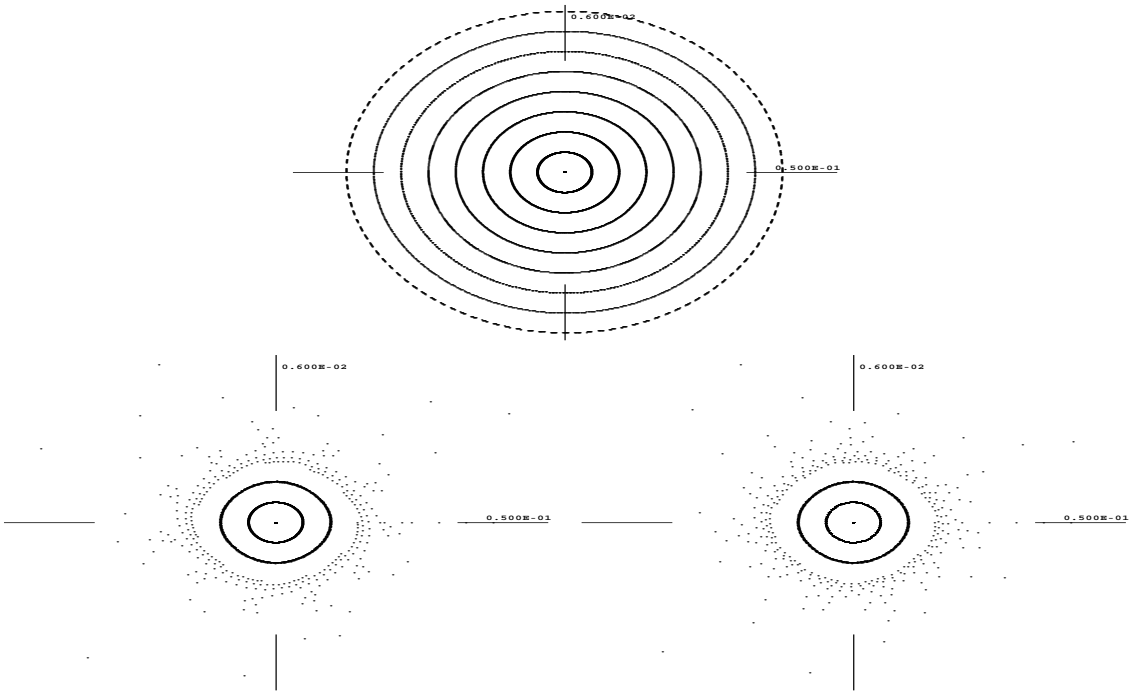

FIGURE 3. Tracking pictures for 1000 turns in a 30GeV neutrino factory ring without (upper) and with (lower) fringe field effects, and further without (left) and with (right) kinematic correction in the same scale of 50mm×6mrad. With fringe field effects, only those particles up to 10mm×1.5mrad survive.

dynamic aperture decreased by a factor of around 100 in x-a, and there is a corresponding large increase in the tune footprint area. To illustrate the other nonlinear effects, pictures in Figure 3 give a glimpse to the consequences of fringe field effects, which are reported in more detail in [2]. The setting of the system is the same to the previous tracking pictures, but with a smaller phase space region. The upper picture shows the situation with kinematic correction, and the particles are stable in this region without the fringe field effects. Now, the lower pictures show the cases with fringe field effects (left), and fringe field effects plus kinematic correction (right). With fringe field effects, the particles survive up to about 10mm×1.5mrad in x-a, which represents a further decrease of the phase space by a factor of 100, and at this scale, the effects of the kinematic correction are relatively suppressed.

The 30 GeV Higgs factory ring was studied in the similar way. Roughly speaking, the amount of effects by those nonlinear corrections is similar to that of the neutrino factory ring.

The tracking pictures in Figure 4 and 5 can be used to estimate the size of the dynamic aperture. Particles were tracked for 1000 turns with transfer maps up to 7th order, and those with x up to 40mm and a up to 300mrad are stable in

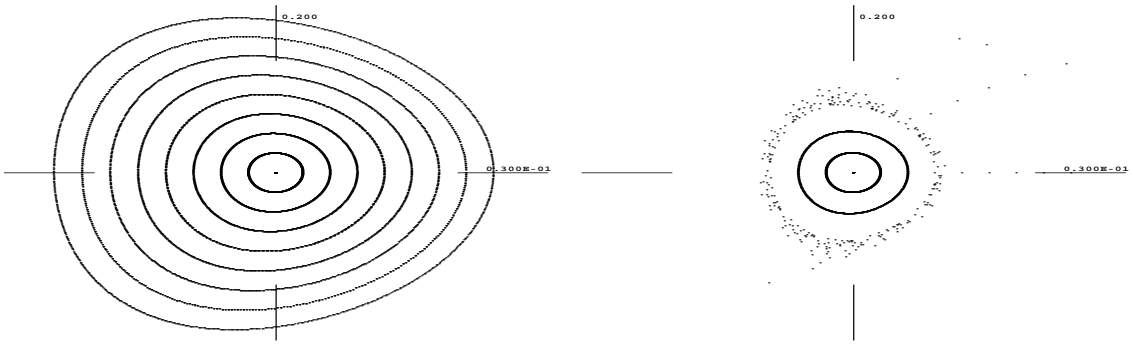

FIGURE 4. Tracking pictures for 1000 turns in a 30 GeV Higgs factory ring without (left) and with (right) kinematic correction in the same scale of 30mm×200mrad. The fringe field effects are not included. With correction, only those particles up to 6mm×50mrad are stable.

the Higgs factory ring when neither kinematic correction nor fringe field effects are included. By turning on only the kinematic correction, the stable size decreased to x up to 6mm and a up to 50mrad, which is a decrease by a factor of 40 in x-a. By including the fringe field effects, a further decrease by a factor of 100 in x-a is observed. However, under the influence of the fringe field effects, the difference between with and without kinematic correction is suppressed.

The amplitude dependent tune shifts are listed in Table 3. Figure 6 shows the tune footprints for particles up to 0.5mm in radius in both x and y directions. The pictures show the comparison with and without kinematic correction, but the fringe field effects are not included. The upper picture shows the tune footprint without the kinematic correction, and the lower picture shows the one with the correction. In the lower picture, the tiny horizontal bar at the lower left is the region of the footprint without the correction for comparison.

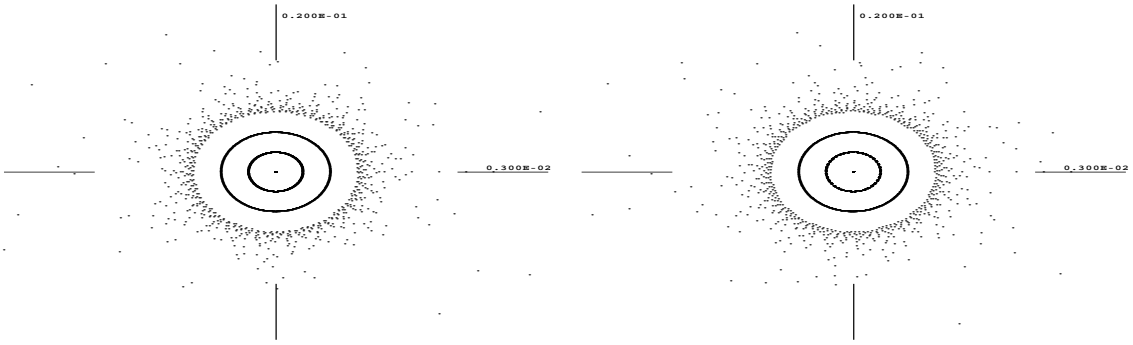

FIGURE 5. Tracking pictures for 1000 turns in a 30 GeV Higgs factory ring under the influence of the fringe field effects in the scale of 3mm×20mrad. Particles up to 0.6mm×5mrad are stable without (left) and with (right) kinematic correction.

Altogether a decrease of the stable region by up to a factor of 100 and an increase of the tune footprint area by up to a factor of 10^5 are observed by the kinematic correction when there is no influence of the fringe field effects.

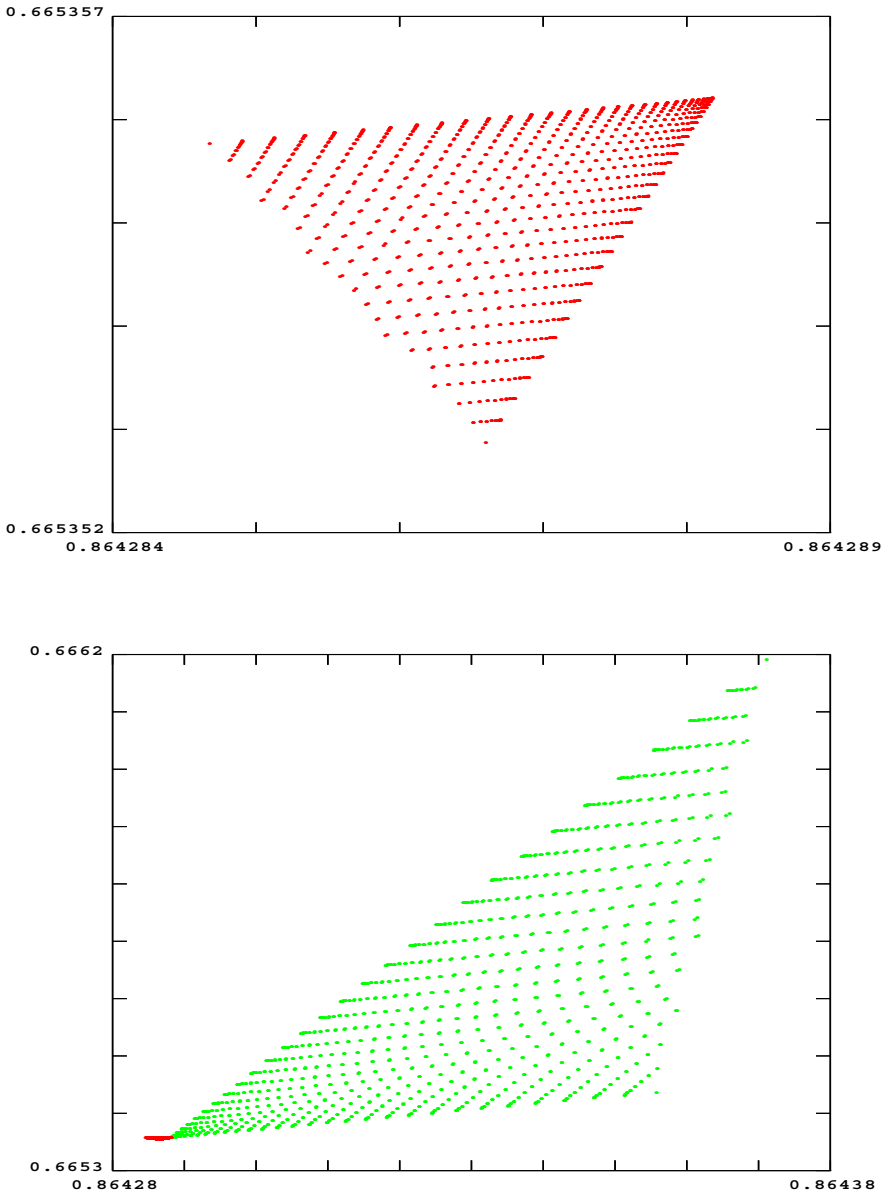

FIGURE 6. Tune footprints of a 30 GeV Higgs factory ring without (upper) and with kinematic correction. The lower picture shows both footprints in the same scale, where the one without correction is the tiny bar at the lower left.

ACKNOWLEDGMENTS

This study was motivated through a discussion with J. Gallardo. We thank C. Johnstone and W. Wan for providing the storage ring designs for the study. The work was supported by the US Department of Energy and the Alfred P. Sloan Foundation.

REFERENCES

1. W. Wan, C. Johnstone, J. Holt, M. Berz, K. Makino, and M. Lindemann. The influence of fringe fields on particle dynamics in the Large Hadron Collider. *Nuclear Instruments and Methods A*, in print.
2. M. Berz, K. Makino, and B. Erdélyi. Fringe field effects in muon rings. In these proceedings.
3. K. Makino. *Rigorous Analysis of Nonlinear Motion in Particle Accelerators*. PhD thesis, Michigan State University, East Lansing, Michigan, USA, 1998. Also MSUCL-1093.
4. M. Berz. COSY INFINITY Version 8 reference manual. Technical Report MSUCL-1088, National Superconducting Cyclotron Laboratory, Michigan State University, East Lansing, MI 48824, 1997. See also http://cosy.nscl.msu.edu.
5. K. Makino and M. Berz. COSY INFINITY version 8. *Nuclear Instruments and Methods*, A427:338, 1999.
6. K. Makino and M. Berz. COSY INFINITY Version 7. In *Fourth Computational Accelerator Physics Conference*, volume 391, page 253. AIP Conference Proceedings, 1996.
7. M. Berz. Computational aspects of design and simulation: COSY INFINITY. *Nuclear Instruments and Methods*, A298:473, 1990.
8. M. Berz, B. Erdélyi, W. Wan and K. Y. Ng. Differential algebraic determination of high-order off-energy closed orbits, chromaticities, and momentum compactions. *Nuclear Instruments and Methods*, A427:310, 1999.
9. M. Berz. *High-Order Computation and Normal Form Analysis of Repetitive Systems, in: M. Month (Ed), Physics of Particle Accelerators*, volume AIP 249, page 456. American Institute of Physics, 1991.
10. M. Berz. Differential algebraic formulation of normal form theory. In *M. Berz, S. Martin and K. Ziegler (Eds.), Proc. Nonlinear Effects in Accelerators*, page 77. IOP Publishing, 1992.